Electronic Supplementary Material (ESI) for ChemComm.

Supplementary information

Towards lithium-free solid-state battery with nanoscale Ag/Cu sputtered bilayer electrodes

*Lorenzo Fallarino[1], Uzair Naveed Chishti[1], Arianna Pesce[1], Grazia Accardo[1], Amna Rafique[1,2,3], Montserrat Casas-Cabanas[1,4] and Pedro López-Aranguren[1,]**

[1]Centre for Cooperative Research on Alternative Energies (CIC energiGUNE), Basque Research and Technology Alliance (BRTA), Alava Technology Park, Albert Einstein 48, 01510 Vitoria-Gasteiz, Spain

[2]University of Basque Country (UPV/EHU), Barrio Sarriena, s/n, Leioa 48940, Spain

[3]ALISTORE-European Research Institute

[4]Ikerbasque, The Basque Foundation for Science, 48013 Bilbao, Spain

*corresponding author, e-mail: plopez@cicenergigune.com

Sample fabrication

Niobium doped LLZO powder from TOSHIMA (d_{50} = 1μm) has been used to prepare the solid electrolytes. An optimized powder amount of w = 0.32 - 0.35 g was uniaxially pressed at 2-ton for 1 min to form a pellet with a diameter of d = 10 mm. For the sintering step, the pellets were placed in alumina crucibles and covered with mother powder of the same material to prevent lithium evaporation at high temperatures. The pellets were sintered at T = 1200 ºC in synthetic air atmosphere for 6 hours with an increasing temperature ramping rate of ΔT = 3 ºC / min. After sintering all pellets were progressively polished by applying 240, 400, 600, 1200 and 2400 grit SiC disks. For reproducibility purposes, all pellets were thinned down to 1 mm. The entire fabrication process of pellets has been performed inside the glovebox ($H_2O \leq 0.5$ ppm and $O_2 \leq 0.5$ ppm), whose atmosphere is saturated by argon (Ar).

PFEIFFER Classic 500 SP sputtering system has been utilized to deposit Ag and Cu thin films onto the pellets. The deposition rates were calibrated by depositing (Cu and Ag) on silicon wafers and the respective thickness was measured by Bruker stylus Profiler DEKTAKXT. The pellets were transferred from the glovebox to the sputtering system by using an airtight transfer arm. The pellets have been mounted between two customized stainless-steel masks, which have been used to protect the lateral sides of the pellets from been coated. The distance between the sputtering targets and the pellets inside the main sputtering chamber was approximately 10 cm. A DC power of 50 W was applied to sputter Cu and 20 W to sputter Ag, under an argon gas pressure of 1×10^{-1} Pa. In addition, to avoid lateral thickness variations, the pellets rotate during the depositions. For the bi-layer systems, the deposition of Ag is immediately followed by the one of Cu. To prevent contamination while sputtering the bilayers, the sputter guns are closed by shutters allowing the deposition of only one material at a time.

Structural characterization of LLZO pellets

Rietveld refinement: the structure of LLZO pellets was determined from x-ray diffraction (XRD) θ/2θ measurements. XRD patterns were recorded using a Bruker D8 Discover diffractometer (monochromatic Cu radiation $\lambda_{Cu,K\alpha_1}$ = 1.54053 Å).

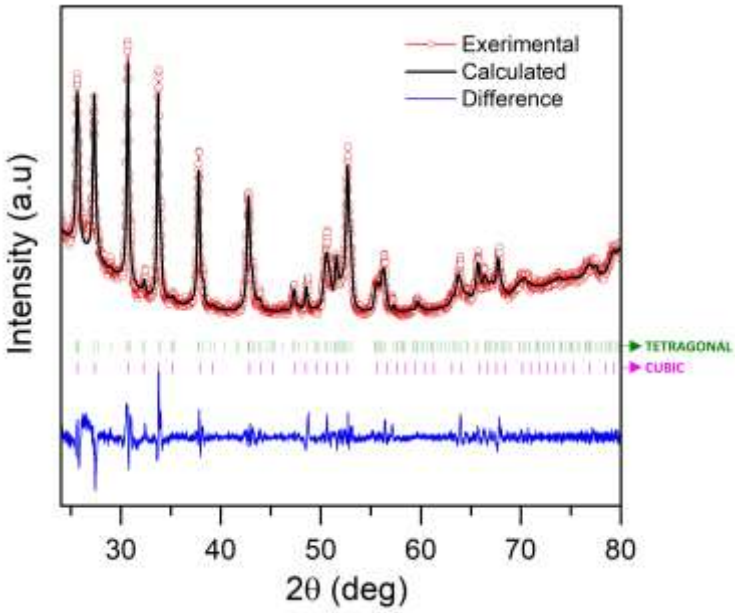

Fig. S1: Rietveld refinement of XRD data of synthesized LLZO pellet. The red open circles and lines represent the experimental result, the black line is the fitting curve; the bars show the Bragg positions of the cubic (pink) and tetragonal (green) phases, and the blue line is the difference between experiment and fitting.

The XRD patterns were refined using the program FullProf [1]. The corresponding Rietveld refinement pattern is shown in Fig. S1 as black solid lines, together with the experimental data (red open circles and solid line), and their difference (blue line). The pattern was indexed on both the cubic space group $Ia\bar{3}d$ and the tetragonal space group $I4_1/acd$. The fitting was satisfactory (R^2 = 0.977, χ^2 = 3.5) providing refined unit cell parameters as: a = b = c = 12.997(7) Å for the cubic phase (66%), a = b = 13.051(5) Å and c = 12.848(5) Å for the tetragonal phase (34%).

Structural stability: the stability of LLZO during cycling and under temperature change has been characterized by XRD before and after cycling, as displayed in Fig. S2. A cell assembled as Li_{foil} | LLZO | Li_{foil} has been used to carry this experiment out. The XRD data have been collected after long cycling and after the removal of Li from both sides. It can be clearly seen that both scans look nearly identical in their overall appearance, exhibiting only well-defined diffraction peaks corresponding to the LLZO electrolyte, confirming the stability of the electrolyte against electrochemical cycling at operating temperature. This was somehow expected since all pellets were sintered at T = 1200 ºC. Consequently, any structural change should not be expected at T = 70 ˚C. It is worth mentioning that the broad peaks at low

diffraction angle, as well as the not-linear background the same angular range, are both coming from the Kapton tape that must be used in order to protect the pellet from the ambient atmosphere during the measurement.

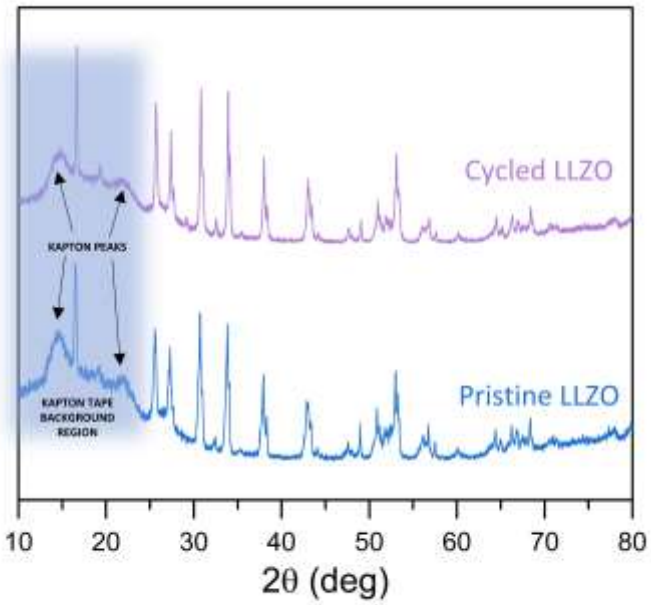

Figure S2: x-ray diffraction θ/2θ measurements of a pristine LLZO pellet (bottom, blue line) and after electrochemical plating and stripping experiments in a symmetric cell configuration Li_{foil} | LLZO | Li_{foil} (top, purple line). The Li_{foil} has been removed from both sides before XRD measuring.

Ag-Li alloy calculations

Via x-ray diffraction peak position: according to the Ag-Li binary phase diagram [2], the alloy shows a series of solid solutions, which can be formed at a wide range of Li atom%. In the range $0 \leq$ Li atom% ≤ 50, the original crystalline structure of Ag should be preserved. Therefore, to calculate the lattice spacing, and consequently the lattice parameter of the Ag-Li alloy, we consider the face-centered-cubic crystalline (*fcc*) structure, which we apply to Bragg's law.

$$n\lambda = 2d \sin\theta, \qquad d(h,k,l) = \frac{a}{\sqrt{h^2+k^2+l^2}} \tag{E1}$$

$$a = \frac{\lambda\sqrt{h^2+k^2+l^2}}{2\sin\theta} \tag{E2}$$

Since we are looking at the (111) diffraction peak, and we are using a Cu-Kα radiation:

$$2\theta = 38.41^\circ, \qquad \lambda_{Cu_{K\alpha 1}} = 0.154\ nm, \qquad h = k = l = 1 \tag{E3}$$

$$a = \frac{0.154\sqrt{3}}{2\sin(19.205^\circ)} = 0.401 \text{ nm} \tag{E4}$$

The lattice parameter as a function of Ag-Li composition [3], is shown in Fig. S3. According to the graph, the alloy corresponding to a = 0.402 nm would be $Ag_{46\pm4}Li_{54\pm4}$. The error has been calculated by propagating the error attributed to the diffraction angle.

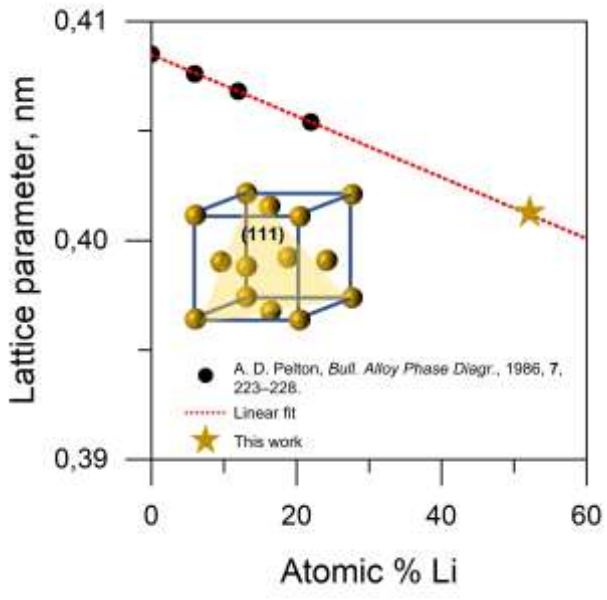

Fig. S3: lattice parameter of the *fcc* crystalline structure of Ag (depicted by the schematic) as a function of the atomic percentage of Li-doping. The (red light) triangle highlights the (111) crystalline plane. The (yellow) spheres correspond to the Ag atoms.

Via electrochemical plating data: according to [4], for every 1 mAh/cm^2 capacity, the thickness of "fresh" deposited Li is measured to be about 5 μm.

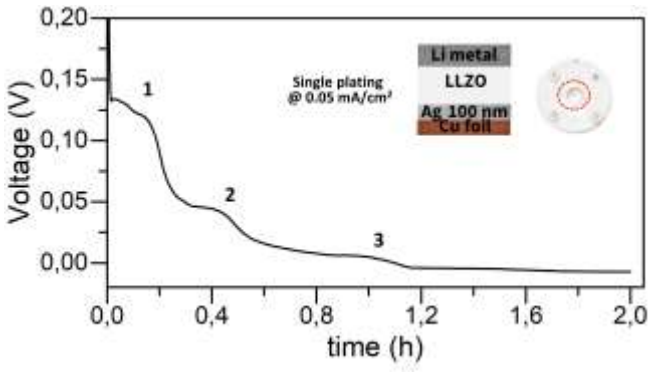

Fig. S4: Voltage profiles of the Li plating at j = 0.1 mA/cm^2 together with a schematic of the Li/LLZO/Ag(100 nm)/Cu_foil cell and a picture of coated pellet by the Ag layer. The sputtering mask is also visible, which was used to avoid coating the lateral part of the pellet.

Three different alloy formation steps (marked in Fig. S4 as 1, 2, and 3) are clearly visible: the first at $t \approx 0.18 \pm 0.03$ h, the second at $t \approx 0.47 \pm 0.05$ h, and the third $t \approx 0.96 \pm 0.11$ h. The position in time has been calculated by taking the dV/dt and by fitting, with single Gaussian function, the peak positions. The attributed errors correspond to half of the FWHM of the peaks. Therefore, the three steps would correspond to: 1 → ≈ 44 ± 7 nm of Li; 2 → ≈ 112 ± 13 nm of Li; 3 → ≈ 242 ± 18 nm of Li.

By using the following formula, and by assuming a layer-like deposition of the Li atoms, and that all Li and Ag atoms participate in the alloy process, the number of Li atoms N can be calculated for the three steps:

$$N(Li) = \frac{N_A \cdot \rho \cdot V}{M_w} \tag{E5}$$

$$N_1 = (1.27 \pm 0.18) \times 10^{17}, N_2 = (4.19 \pm 0.50) \times 10^{17}, N_3 = (10.46 \pm 0.85) \times 10^{17}$$

By using the same formula, we can calculate the number of Ag atoms within the 100 nm thickness:

$$N(Ag) = \frac{N_A \cdot \rho \cdot V}{M_w} = 5.83 \times 10^{17} \tag{E6}$$

By assuming a 100% efficiency of the alloying process, and that Li and Ag share the same surface area, the first alloy step would then correspond to Ag → $Ag_{86\pm2}Li_{14\pm2}$, the second to $Ag_{86\pm2}Li_{14\pm2}$ → $Ag_{58\pm6}Li_{42\pm6}$, and the third to $Ag_{58\pm6}Li_{42\pm6}$ → $Ag_{37\pm6}Li_{63\pm6}$. The error has been calculated by propagating the error attributed to the peak position of the dV/dt, calculated as

the FWHM of the peaks. It is worth mentioning that these and the previous calculations do not pretend to be exact, but just to be a guidance for the stoichiometry evolution of the alloy formation.

Electrochemistry

Electrochemical characterization: the cells have been assembled in a Swagelok configuration. Li metal disks of 4 mm diameter were applied as positive electrodes. The solid electrolytes sandwiched between the Li metal electrode and the sputtered Ag/Cu bilayer current collector were slightly pressed using a hydraulic press to plastically deform the Li, and, consequently, to decrease its thickness and to increase the active area with the garnet oxide electrolyte. All electrochemical experiments have been performed at T = 70º C in a climactic chamber. A cut-off voltage of $V_{cut\text{-}off}$ = 1 V was established in the stripping step to avoid reaching the safety limit of the experimental setup.

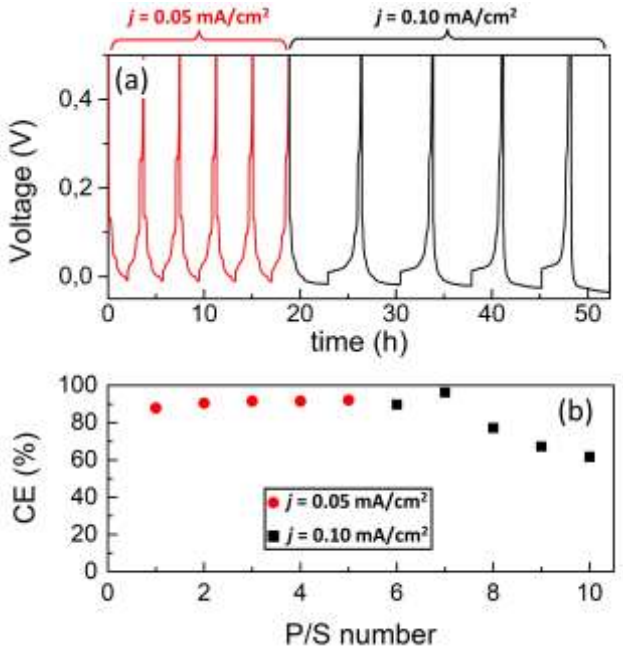

Figure S5: (a) potential response of a Li/LLZO/Ag(100nm)/Cu(600nm) after plating and stripping at j = 0.05 mA/cm^2 (in red) and at j = 0.10 mA/cm^2 (in black). (b) Coulombic efficiency versus cycle number: the (red) dots correspond to current density of j = 0.05 mA/cm^2, whereas the (black) squares refer to j = 0.10 mA/cm^2.

Electrochemical Impedance Spectroscopy: it was performed using a VMP3 module, with AC in a frequency range of 10 kHz to 1 Hz and a bias voltage of 10 mV at T = 70° C.

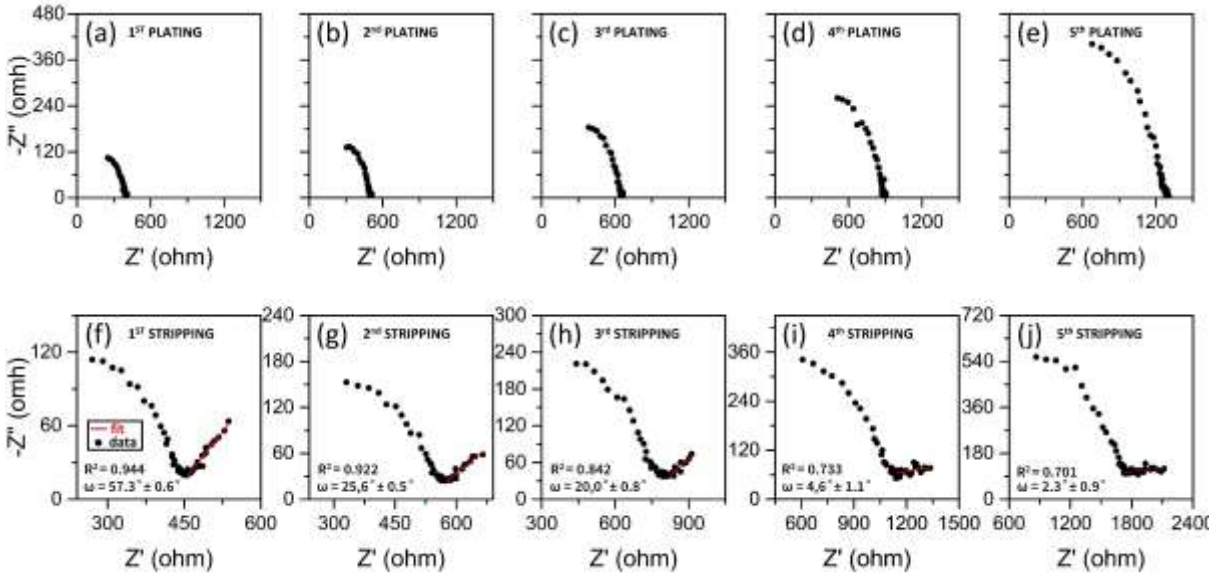

Figure S6: Impedance spectra of a Li/LLZO/Ag(100 nm)/Cu(600nm) sample after the first (a), second (b), third (c), fourth (d), and fifth (e) 2-hour-plating cycle by applying a current density j = 0.10 mA/cm^2. Impedance spectra after the first (f), second (g), third (h), fourth (i), and fifth (j) 2-hour-stripping cycle by applying a current density j = 0.10 mA/cm^2. In (f)-(j) the (red) lines show least-squares fits to a linear function for each of the sample data sets.

Top-view SEM micrographs: they have been recorded by using a Quanta 200 FEG high-resolution microscope in high vacuum. A transfer chamber has been utilized to transfer the sample from the glovebox into the microscope.

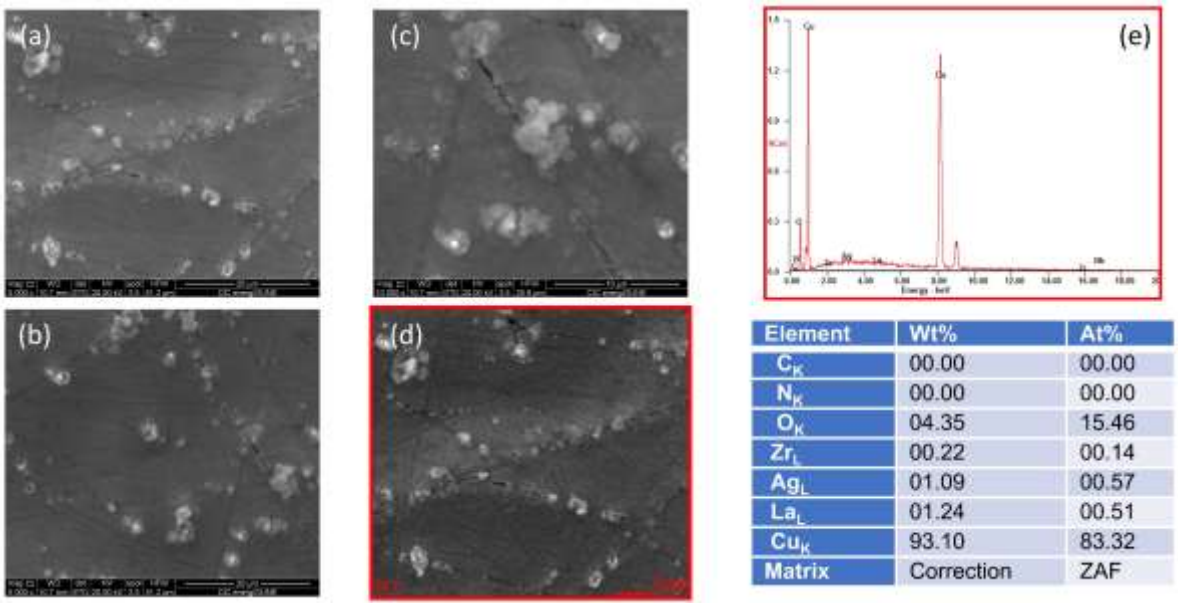

Element	Wt%	At%
C_K	00.00	00.00
N_K	00.00	00.00
O_K	04.35	15.46
Zr_L	00.22	00.14
Ag_L	01.09	00.57
La_L	01.24	00.51
Cu_K	93.10	83.32
Matrix	Correction	ZAF

Figure S7: (a) – (d) Ex situ SEM micrographs of the Cu surface after 5 plating/stripping cycles at j = 0.05 mA/cm^2 plus 5 plating/stripping cycles at j = 0.10 mA/cm^2. (e) EDX analysis of (d), whose results are listed in the table below.

[1] J. Rodriguez-Carvajal, Program FullProf Suite. Available athttp://www.ill.eu/sites/fullprof/; J. Rodríguez-Carvajal, Physica B: Condensed Matter 192, 55–69, 1993.
[2] Y. Fang, S. L. Zhang, Z.-P. Wu, D. Luan, and X. W. Lou, Sci. Adv. 2021, **7**, eabg3626.
[3] A. D. Pelton, Bull. Alloy Phase Diagr., 1986, **7**, 223–227.
[4] S. Chen, C. Niu, H. Lee, Q. Li, L. Yu, W. Xu, J.-G. Zhang, E. J. Dufek, M. S. Whittingham, S. M., J. Xiao, and J. Liu, Joule 3, 1094–1105, 2019.